

# Probing Legacy and Alternative Flame Retardants in the Air of Chinese Cities

Shizhen Zhao, Lele Tian, Zehao Zou, Xin Liu, Guangcai Zhong, Yangzhi Mo, Yan Wang, Yankuan Tian, Jun Li, Hai Guo, and Gan Zhang\*



Cite This: *Environ. Sci. Technol.* 2021, 55, 9450–9459



Read Online

ACCESS |



Metrics & More

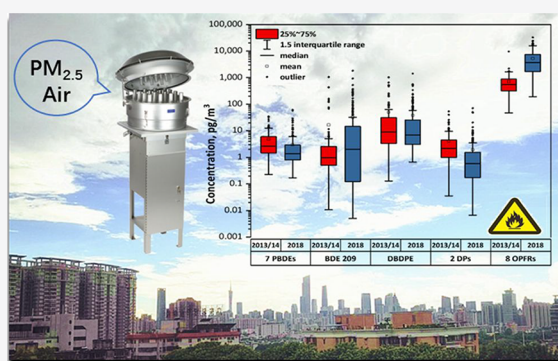


Article Recommendations



Supporting Information

**ABSTRACT:** An increasing number of alternative flame retardants (FRs) are being introduced, following the international bans on the use of polybrominated diphenyl ether (PBDE) commercial mixtures. FRs' production capacity has shifted from developed countries to developing countries, with China being the world's largest producer and consumer of FRs. These chemicals are also imported with e-waste to China. Therefore, it is important to understand the current status of regulated brominated FRs, their phase-out in China, and their replacement by alternatives. In this study, a broad suite of legacy and alternative FRs, including eight PBDEs, six novel brominated FRs (NBFRs), two dechlorane plus variants (DPs), and 12 organophosphate FRs (OPFRs) were evaluated in the air of 10 large Chinese cities in 2018. OPFRs are the most prevalent FRs in China, exhibiting a wide range of 1–612 ng/m<sup>3</sup>, which is several orders of magnitude higher than PBDEs (1–1827 pg/m<sup>3</sup>) and NBFRs (1–1428 pg/m<sup>3</sup>). BDE 209 and DBDPE are the most abundant compounds in brominated FRs (>80%). The North China Plain (NCP, excluding Beijing), Guangzhou, and Lanzhou appear to be three hotspots, although with different FR patterns. From 2013/2014 to 2018, levels of PBDEs, NBFRs, and DPs have significantly decreased, while that of OPFRs has increased by 1 order of magnitude. Gas-particle partitioning analysis showed that FRs could have not reached equilibrium, and the steady-state model is better suited for FRs with a higher log *K*<sub>OA</sub> (>13). To facilitate a more accurate FR assessment in fine particles, we suggest that, in addition to the conventional volumetric concentration (pg/m<sup>3</sup>), the mass-normalized concentration (pg/g PM<sub>2.5</sub>) could also be used.



## INTRODUCTION

Polybrominated diphenyl ethers (PBDEs) are an important class of flame retardants (FRs), widely used in commercial products since the 1970s. During the past decades, they have been a focus of concern due to their high persistence, bioaccumulation, and potential health effects.<sup>1</sup> Three primary PBDE commercial mixtures were gradually banned from use or voluntarily phased out of manufacturing. Penta and octa-BDE mixtures were listed in Stockholm Convention in 2008, and deca-BDE was added in 2017.<sup>2</sup> These regulations facilitated a significant shift from PBDE use toward alternative FRs, such as novel brominated and organophosphate flame retardants (NBFRs and OPFRs).<sup>3</sup> However, these phase-outs and restrictions have been only applied to the newly manufactured products but not to PBDE-containing products and materials already in use.<sup>4</sup>

Many alternative FRs are also halogenated with chemical structures similar to PBDEs. For instance, decabromodiphenyl ethane (DBDPE) is similar to BDE 209.<sup>5</sup> Though little is known about their use or production, they have been widely detected in remote places with an increasing trend, such as the Arctic<sup>6</sup> and Antarctica,<sup>7,8</sup> reflecting their strong long-range atmospheric transport (LRAT) potential.<sup>1</sup> Several studies have revealed that

NBFRs are bioaccumulative in aquatic and terrestrial food chains and that adverse effects have been observed in humans.<sup>9,10</sup> In 2019, DBDPE and dechlorane plus (DPs) were added to Schedule 1 of the toxic substances list published by the Canadian government.

OPFRs are organic esters of phosphoric-acid-containing alkyl chains or aryl groups and function as another important replacement for PBDEs. They are categorized as either halogenated or nonhalogenated.<sup>11</sup> Currently, OPFRs are the most frequently detected FRs in the environment, typically observed at much higher levels than PBDEs' and NBFRs' peaks because of market demand.<sup>12,13</sup> Toxicity testing, epidemiological studies, and risk assessment results indicate that there are

**Special Issue:** POPs on the Global Scale: Sources, Distribution, Processes, and Lessons Learned for Chemicals Management

**Received:** October 31, 2020

**Revised:** March 3, 2021

**Accepted:** March 3, 2021

**Published:** March 23, 2021



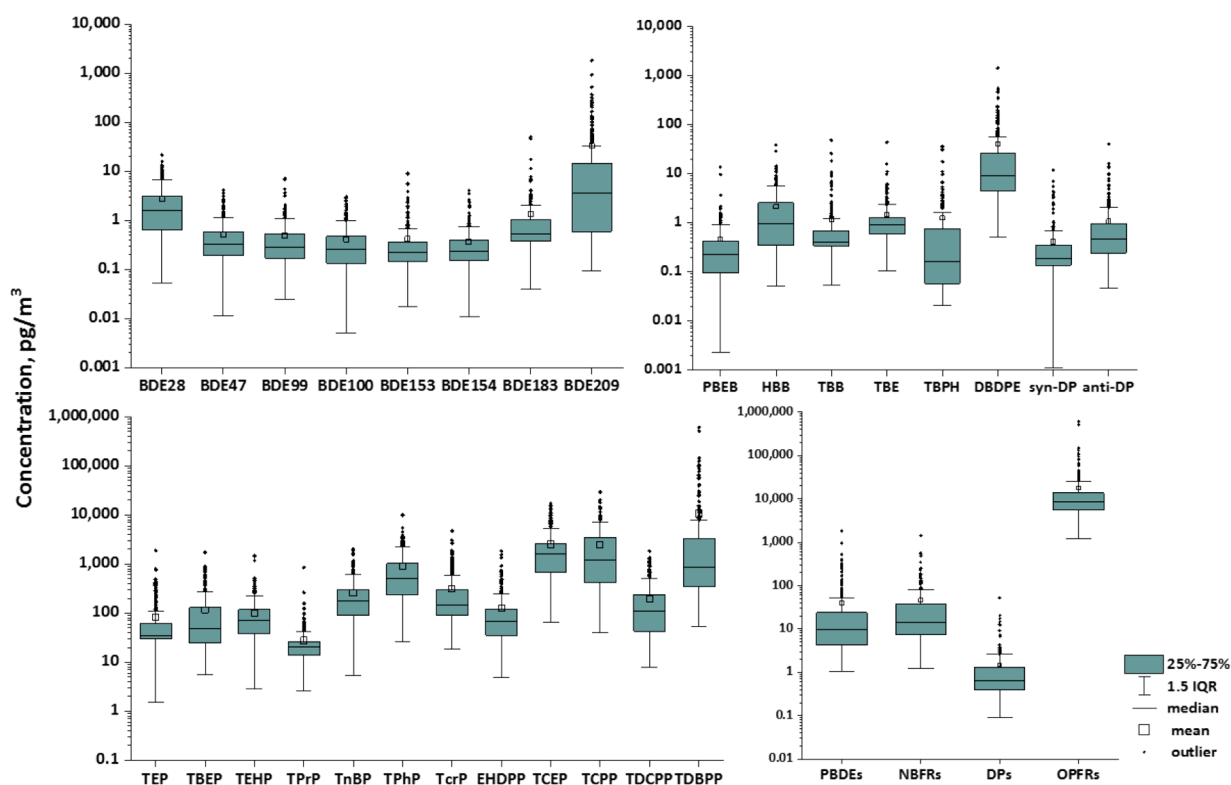


**Figure 1.** Atmospheric profiles (QFF + PUF) of  $\sum_8$  PBDEs,  $\sum_6$  NBFRs,  $\sum_2$  DPs, and  $\sum_{12}$  OPFRs from 10 cities in China ( $n = 274$ ). IQR is the interquartile range.

significant health concerns associated with OPFRs exposure,<sup>1,11</sup> leading it to be criticized as a “regrettable substitution.”<sup>11</sup>

Air is an ideal sampling matrix for monitoring chemical pollution in the ambient environment, because it is well-mixed and economically viable for analysis. In the past decade, several national air sampling campaigns have been launched to monitor PBDEs in China, notably in 2008–2009<sup>14</sup> and 2013–2014.<sup>12</sup> Since then, however, policies related to chemical regulation have been updated internationally and in China. Excluding the later inclusion of BDE 209 to the Stockholm list, the import of e-waste has been strictly banned in China since January 1, 2018, which was previously an important pathway by which FRs entered the country. Moreover, following the successful implementation of the “Air Pollution Prevention and Control Action Plan” (APPCAP) in 2013, air quality across China has greatly improved within the past five years, specifically exhibiting a significant reduction in  $PM_{2.5}$ .<sup>15</sup> These findings indicate scope for further investigation regarding the combined impact of such regulations on the current FR profiles in the air of China.

In this study, we investigated a broad suite of FRs, including eight PBDEs, six NBFRs, two DPs, and 12 OPFRs in air samples from 10 large cities across China. We aimed to (i) investigate the level, pattern, spatial distribution, and temporal trend of typical FRs in the air of Chinese cities; (ii) explore the main factors affecting their distribution in China; and (iii) understand the effectiveness of the current regulation of legacy PBDEs and provide guidance for developing a more effective policy for controlling emerging contaminants in the future. To our knowledge, this is the first comprehensive national-scale FR data set, covering both gaseous and particulate phases, with the most updated information on the current status of legacy FRs, their phase-out from the Chinese market, and their replacement by alternatives.

## ■ MATERIALS AND METHODS

**Nationwide Sampling Campaign.** Ten provincial capital cities were selected for analysis across China: Beijing, Shanghai, Guangzhou, Wuhan, Guiyang, Shijiazhuang, Lanzhou, Jinan, Chengdu, and Zhengzhou. An urban site and a rural site were set up in each city, based on the network of official air monitoring stations and following the suggested criteria,<sup>16</sup> which are representative of the city-level air pollution characteristics. In general, the urban site is in the central urban area of the city, while the suburban site is in the peripheral region outside the central city. At each site, a high-volume active air sampler at a sampling rate of 1 m<sup>3</sup>/min (Minya Instruments Co., Guangzhou, China) was fitted with a polyurethane foam plug (PUF, 6.2 cm in diameter, 7.8 cm in thickness, and 0.030 g/cm<sup>3</sup> in density) and a quartz fiber filter (QFF, Whatman, 203 mm × 254 mm), to capture FRs in gaseous and  $PM_{2.5}$  phases. Air samples were collected continuously every 24 h for 1 week in winter (January 2018) and summer (July 2018). A total of 280 paired samples were retrieved. Detailed sampling information is presented in Table S1. Before sampling, QFFs were baked at 450 °C overnight, and PUFs were precleaned separately with acetone and dichloromethane. All samples were delivered in ice bags to the lab and stored at −20 °C before analysis.

**Sample Pretreatment and Analysis.** Sample treatment and instrumental analysis were conducted as described in our previous studies<sup>12,17</sup> as shown in Text S1. The 28 target FRs evaluated in this study are detailed in Table S2. Briefly, QFFs and PUFs were spiked with recovery surrogates (<sup>13</sup>C<sub>12</sub>-PCB 155/206, TnBP-*d*<sub>27</sub>, and TDCPP-*d*<sub>15</sub>) and Soxhlet extraction. The extracts were then concentrated and purified via multilayer silica gel column chromatography, and the internal standards were added before instrumental analysis. The selected

monitoring ions and retention times are shown in Tables S3 and S4.

**Quality Assurance and Quality Control (QA/QC).** QA/QC was conducted using field blanks, procedural blanks, and surrogate spiked recoveries. The average recovery rates were  $75 \pm 13\%$  for  $^{13}\text{C}_{12}$ -PCB 155,  $85 \pm 22\%$  for  $^{13}\text{C}_{12}$ -PCB 206,  $86 \pm 21\%$  for TnBP- $d_{27}$ , and  $51 \pm 11\%$  for TDCPP- $d_{15}$ . The reported concentrations were corrected for blanks and surrogate recoveries. The method detection limits (MDLs) and instrumental detection limits (IDLs) of the target compounds are listed in Tables S5 and S6.

**Gas-Particle Partitioning.** Organic compounds' distribution between gas-particle (G/P) phases in the air is generally explained by using the G/P partition coefficient.<sup>18</sup> We employed three widely used approaches, the steady-state Li-Ma-Yang model,<sup>19</sup> the  $K_{\text{OA}}$ -based model assuming equilibrium conditions,<sup>18</sup> and its corresponding empirical model<sup>19</sup> to predict the G/P partition quotient of FRs,<sup>20</sup> as detailed in Text S2. Only FRs detected in both phases of a given sample were included.

## RESULTS AND DISCUSSION

**General Profiles.** The minimum, maximum, and median concentrations of selected FRs are summarized in Tables S7 and S8 and Figure 1. The atmospheric levels of  $\sum_8$  PBDEs,  $\sum_6$  NBFrs,  $\sum_2$  DPs, and  $\sum_{12}$  OPFRs in air samples ( $n = 274$ ) ranged widely between 1 and 1826  $\text{pg}/\text{m}^3$ , 1 and 1428  $\text{pg}/\text{m}^3$ , < MDL-53  $\text{pg}/\text{m}^3$ , and 1 and 612  $\text{ng}/\text{m}^3$ . The median level ranked as  $\sum_{12}$  OPFRs (9  $\text{ng}/\text{m}^3$ )  $\gg$   $\sum_6$  NBFrs (14  $\text{pg}/\text{m}^3$ )  $>$   $\sum_8$  PBDEs (10  $\text{pg}/\text{m}^3$ )  $>$   $\sum_2$  DPs (1  $\text{pg}/\text{m}^3$ ). Their concentration distributions were all highly skewed, varying by several orders of magnitude, suggesting emission variability. Most Spearman correlations between different pairwise FRs were significantly positive, as shown in Table S9, suggesting the continued emission of phasing-out substances and similar environmental behavior of replacement substances.<sup>17</sup>

**PBDEs.** The sum of BDE 28, 47, 99, 100, 153, 154, and 183 is expressed as  $\sum_7$  PBDEs. The detection frequencies of  $\sum_7$  PBDEs and BDE 209 were 86–96% and 74% in the  $\text{PM}_{2.5}$  phase, respectively, while they were 32–98% and 36% in the gaseous phase, respectively. This indicated that  $\sum_7$  PBDEs remain ubiquitous in ambient air, despite having been banned for over 10 years.  $\sum_7$  PBDEs in the gaseous phase ranged from <MDL to 23  $\text{pg}/\text{m}^3$  ( $3 \pm 4$   $\text{pg}/\text{m}^3$ ), while that in the  $\text{PM}_{2.5}$  ranged from 1 to 62  $\text{pg}/\text{m}^3$  ( $3 \pm 6$   $\text{pg}/\text{m}^3$ ). BDE 209 dominated the atmospheric  $\sum_8$  PBDEs with an average of  $47 \pm 32\%$ , and BDE 28 ranked second ( $25 \pm 22\%$ ). BDE 28 exhibited the highest level comprising  $\sim 60\%$  of  $\sum_7$  PBDEs in the gaseous phase followed by BDE 183 (11%) and BDE 47 (10%), whereas BDE 183 prevailed (30%) in the  $\text{PM}_{2.5}$  phase followed by BDE 28 (15%). The PBDE levels in our study are comparable to those of studies in Dalian<sup>21</sup> and Beijing,<sup>22</sup> 1–2 orders of magnitude lower than those reported in eight cities of Pakistan averaged at 172  $\text{pg}/\text{m}^3$ ,<sup>3,23</sup> and 20 big cities globally averaged at 42  $\text{pg}/\text{m}^3$ ,<sup>16</sup> as summarized in Table S10.

The BDE 209 concentrations in  $\text{PM}_{2.5}$  were between <MDL and 1820  $\text{pg}/\text{m}^3$  ( $32 \pm 135$   $\text{pg}/\text{m}^3$ ) and were at a lower level of <MDL-34  $\text{pg}/\text{m}^3$  ( $1 \pm 3$   $\text{pg}/\text{m}^3$ ) in the gaseous phase. In Figure S1, winter samples showed a much higher BDE 209 level ( $63 \pm 146$   $\text{pg}/\text{m}^3$ ) than those in summer ( $15 \pm 27$   $\text{pg}/\text{m}^3$ ). BDE 209 levels in our study are similar to those of the 10-city study in China ( $31 \pm 150$   $\text{pg}/\text{m}^3$ )<sup>19</sup> and the global study (28  $\text{pg}/\text{m}^3$ )<sup>16</sup> but higher compared to those in Chicago ( $11 \pm 2$   $\text{pg}/\text{m}^3$ ).<sup>24</sup> China began producing deca-PBDEs in the 1980s and became

the major global manufacturer by the 2000s.<sup>25</sup> As the stock of commercial penta- and octa-BDE in existing products gradually declines, BDE-209 is becoming more important as a continuous source of PBDEs in China. In the United States and Canada, it was estimated that approximately 60% of the BDE-209 stock in 2014 could be in use until 2020.<sup>4</sup> However, in China, the accurate remaining stock of PBDEs remains unknown.

**Novel Brominated Flame Retardants (NBFrs).** The detection frequencies of six NBFrs ranged at 57–92% in the particulate phase and 10–85% in the gaseous phase.  $\sum_6$  NBFr concentration in the gaseous phase ranged from 1 to 406  $\text{pg}/\text{m}^3$  ( $8 \pm 27$   $\text{pg}/\text{m}^3$ ), while it ranged from 1 to 1412  $\text{pg}/\text{m}^3$  ( $38 \pm 108$   $\text{pg}/\text{m}^3$ ) in  $\text{PM}_{2.5}$ . The dominant compounds in the particulate phase were DBDPE ( $71 \pm 22\%$ ) and hexabromobenzene (HBB,  $12 \pm 16\%$ ), whereas DBDPE ( $61 \pm 20\%$ ) and 1,2-bis(2,4,6-tribromophenoxy)ethane (TBE) dominated ( $12 \pm 16\%$ ) in the gaseous phase. A higher level of  $\sum_6$  NBFrs ( $72 \pm 150$   $\text{pg}/\text{m}^3$ ) was observed in winter compared to summer ( $19 \pm 30$   $\text{pg}/\text{m}^3$ ). DBDPE was the most abundant compound in  $\sum_6$  NBFrs in both phases, with a wide range of 1–1141  $\text{pg}/\text{m}^3$  ( $39 \pm 108$   $\text{pg}/\text{m}^3$ ). Significant seasonality was observed for DBDPE concentrations, which was high during winter ( $63 \pm 146$   $\text{pg}/\text{m}^3$ ) and lower in summer ( $5 \pm 27$   $\text{pg}/\text{m}^3$ ). Their levels were double those in Dalian<sup>21</sup> and Pakistan<sup>23</sup> but comparable to the global study,<sup>16</sup> as shown in Table S11.

DBDPE is widely used as an alternative to BDE-209 in various polymeric materials,<sup>1</sup> such as manufacturing electrical and electronic equipment (EEE).<sup>26</sup> DBDPE production capacity could have been transferred to China because of its restriction in developed countries.<sup>26</sup> China contributed >50% of total global DBDPE production in 2012.<sup>27</sup> In 2014, the annual DBDPE production was double that of deca-BDE in China.<sup>26</sup> As one of the world's largest EEE importers, a large volume of DBDPE is expected to enter China via DBDPE-containing EEE from developed countries.<sup>26</sup> In this study, DBDPE (42%) contributed double of what BDE 209 (20%) contributed to the total halogenated FRs. In contrast, the DBDPE level was much lower than that of BDE 209 in Pakistan,<sup>23</sup> indicating varied usage patterns.

The total  $\sum_5$  NBFrs concentration (excluding DBDPE) was lower, ranging from 2 to 134  $\text{pg}/\text{m}^3$  ( $12 \pm 14$   $\text{pg}/\text{m}^3$ ), because of their minimal production and use in China (Figure 1). In this study, the ratios of 2-ethylhexyl-2,3,4,5-tetrabromo-benzoate (TBB) and bis(2-ethylhexyl)-tetrabromophthalate (TBPH) averaged at  $5 \pm 6$ , which are higher than that in the Firemaster 550 commercial mixture (4:1 by mass),<sup>5</sup> and previous report on American indoor dust averaged at 4.4,<sup>5</sup> suggesting diverse sources with different chemical compositions, fates, and transport mechanisms from emission products. Limited information on their production and usage is available in China, although this is considered insignificant due to their low concentrations.

A mixture of TBPH and TBB, TBE, and DBDPE are used as alternatives to penta-BDE, octa-BDE, and deca-BDE mix formulations, respectively.<sup>17</sup> Strong positive correlations were observed between legacy FRs and their replacements in the air of China, including pairs of DBDPE and BDE 209, TBB and TBPH, and a (TBPH + TBB) and penta-BDE mix (Spearman  $r^2 = 0.30$ – $0.51$ ,  $p < 0.001$ ), as shown in Figure S2, suggesting similar drivers controlling their spatial distribution. This is consistent with previous studies on Chinese forest soils<sup>17</sup> and the air over the Great Lakes.<sup>28</sup>

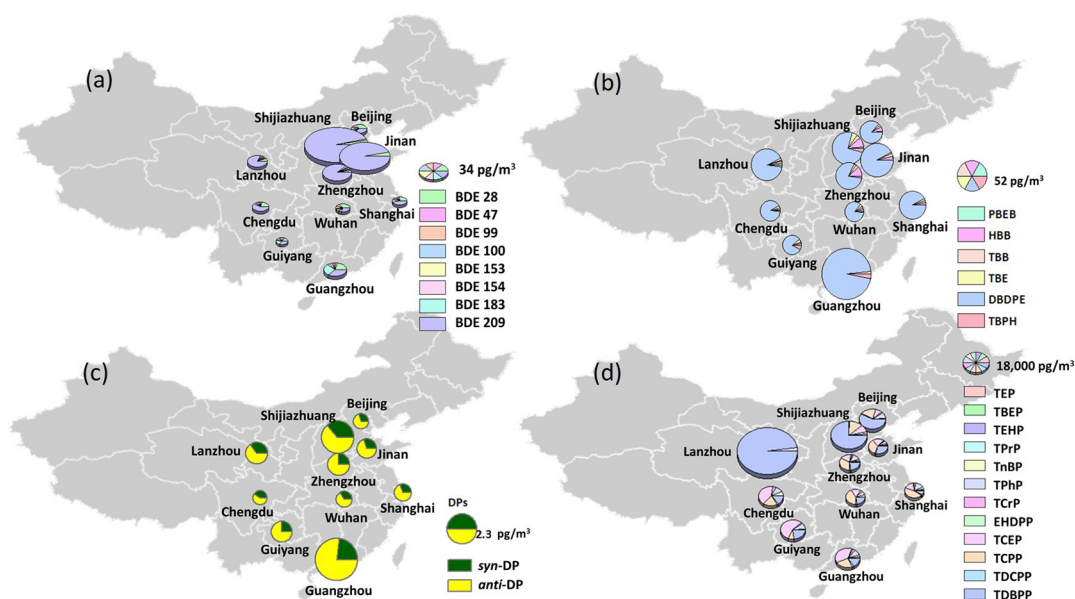


**Figure 2.** Spatial distribution of  $\sum_8$  PBDEs (a),  $\sum_6$  NBRFRs (b),  $\sum_2$  DPs (c), and  $\sum_{12}$  OPFRs (d) across 10 Chinese cities. This figure was modified from the output of ArcGIS 10.3 software, and the base map of China was from <http://www.arcgisonline.cn>.

**Dechlorane Plus (DPs).** DPs are highly chlorinated and composed of two stereoisomers (*syn*-DP and *anti*-DP) in commercial products, as a substitute for Dechlorane (also called Mirex) since the 1970s.<sup>29</sup> In our study, low levels of atmospheric DPs ranged between 0.1 and 53  $\text{pg}/\text{m}^3$  ( $1.5 \pm 3.8 \text{ pg}/\text{m}^3$ ) and mainly existed in the  $\text{PM}_{2.5}$  phase ( $66\% \pm 25\%$ ), dominated by *anti*-DP ( $\sim 60\%$ ). The total *anti*-DP concentration averaged at  $0.4 \pm 1.0 \text{ pg}/\text{m}^3$ , while that of *syn*-DP was  $1.1 \pm 2.9 \text{ pg}/\text{m}^3$ . Winter exhibited significantly higher concentrations of both *syn*-DP and *anti*-DP than summer (Mann–Whitney  $t$  test,  $p < 0.001$ ). In the past decade, a significantly decreasing DP trend has been observed (Table S12). Our measured DPs were an order of magnitude lower than those in a national air study ( $\sim 15 \text{ pg}/\text{m}^3$ ) sampled in 2005,<sup>30</sup> and in northeast China ( $\sim 7 \text{ pg}/\text{m}^3$ )<sup>31</sup> between 2008 and 2013. However, it was comparable to those in the global atmosphere during 2005–2006 ( $\sim 1 \text{ pg}/\text{m}^3$ ).<sup>32,33</sup> Apparently, the current DP levels in Chinese cities are in a low range.

The isomeric DP composition is a useful tool for tracking their source and environmental processes. The fractional abundance ( $F_{\text{anti}}$ ) is defined as the *anti*-isomer concentration divided by the summed DP concentrations. The  $F_{\text{anti}}$  value calculated from the total concentration was  $0.69 \pm 0.10$  (0.30–0.99) without seasonality. The ratio was  $0.72 \pm 0.11$  and  $0.61 \pm 0.16$  in particulate and gaseous phases, respectively, which reflects those of commercial DP products, such as Anpon (0.60) and OxyChem (0.80–0.64).<sup>34</sup> The  $F_{\text{anti}}$  value from our study is higher than the previously reported value of  $0.54 \pm 0.07$  in the particulate phase,<sup>12</sup> similar to the result of a national study in 2005 ( $\sim 0.67$ ).<sup>30</sup> *Syn*-DP was highly correlated to the *anti*-DP (Spearman  $r = 0.874$ ,  $p < 0.001$ ), indicating similar sources. The high  $F_{\text{anti}}$  from this study could indicate that measured DPs are mainly from local emissions instead of LRAT.

**Organophosphate Flame Retardants (OPFRs).**  $\sum_{12}$  OPFRs showed variable detection frequencies between 38 and 93% in the gaseous phase and 43 and 99% in the particulate phase, indicating their ubiquity in ambient air.  $\sum_{12}$  OPFRs' concentration widely ranged between 1 and 612  $\text{ng}/\text{m}^3$  ( $17 \pm 51 \text{ ng}/\text{m}^3$ ), predominantly owing to halo-OPFRs (77%, sum of

tris(2-chloroethyl) phosphate (TCEP), tris(2-chloroisopropyl) phosphate (TCPP), tris(1,3-dichloro-2-propyl) phosphate (TDCPP) and followed by aryl-OPFRs (20%). TDBPP dominated in both phases (27%), followed by TCPP (24%) and TCEP (23%). Our result was 1–2 orders of magnitude higher than those in the Beijing–Tianjin–Hebei region of China,<sup>35</sup> Izmir of Turkey,<sup>36</sup> and Stockholm of Sweden<sup>37</sup> but similar to Pakistan ( $\sim 25 \text{ ng}/\text{m}^3$ ),<sup>23</sup> as summarized in Table S13.

In this study, a high atmospheric TDBPP level ranging from <MDL to 61  $\text{ng}/\text{m}^3$  ( $11 \pm 52 \text{ ng}/\text{m}^3$ ) was observed. It is a widely used flame retardant additive for textiles. After it was reported to be carcinogenic and genotoxic, it became obsolete in markets in the United States and many countries in Europe and has been considered unused since 1970.<sup>38</sup> Therefore, the TDBPP occurrence in the environment has rarely been reported. Recently, it was observed to have a high concentration of a maximum of 9  $\text{mg}/\text{g}$  in the dust collected from California homes.<sup>39</sup> TDBPP ( $\sim 48\%$ ) is the most abundant OPFR compound in the legacy site of Michigan Chemical, which produced this chemical 40 years ago.<sup>40</sup> It has also been widely detected at 100–200  $\text{pg}/\text{L}$  in Arctic rivers,<sup>41</sup> indicating its LRAT potential.

Three chlorinated OPFRs (Cl-OPFRs), TCEP, TCPP, and TDCPP, are mainly used in polyurethane foams, as replacements for the penta-BDE mix.<sup>39</sup> TECP and TCPP had similar atmospheric levels with an average of 3  $\text{ng}/\text{m}^3$ , while TDCPP was an order of magnitude lower than <MDL-0.2  $\text{ng}/\text{m}^3$  ( $0.2 \pm 0.3 \text{ ng}/\text{m}^3$ ). Although TCPP has recently become a worldwide alternative for the more toxic TCEP,<sup>42</sup> they both had comparable levels in our data set. We also observed significant positive correlations among TCEP, TCPP, and TDCPP in Table S9 (Spearman  $r = 0.486$ – $0.796$ ,  $p < 0.001$ ), as their extensive usage and similar sources across China reveal. Three Cl-OPFRs were restricted and regulated in several developed countries. For instance, TDCPP was voluntarily withdrawn from the manufacturing of children's pajamas in the United States and Canada after its metabolites were found to be mutagenic.<sup>43</sup> Both TCEP and TCPP have been listed as carcinogens under

California's Proposition 65.<sup>39</sup> Thus, far, China still lacks policy and regulation controlling these halo-OPFRs.

**Spatial Distribution.** In this study, the intraurban variability of FR patterns was very similar, suggesting similar usage and/or emission patterns on an intraurban scale. This also indicated that selected sampling sites for each city were representative. Therefore, the average level of urban and suburban sites of each city was presented and further discussed on a national scale, as shown in Figure 2. Diverse patterns observed in the Chinese cities and three "hotspots" were identified: the North China Plain (NCP, excluding Beijing), Guangzhou, and Lanzhou. The NCP is one of the most polluted regions in China characterized by high levels of fine particles (e.g.,  $PM_{2.5}$ ) in the atmosphere, because of the large amount of emitted pollutants and the occurrence of unfavorable meteorological situations.<sup>44</sup> The average BDE 209 level in NCP cities (Shijiazhuang, Tianjin, Zhengzhou, and Jinan), was an order of magnitude higher than that in other cities (annual average: 97 vs 7  $pg/m^3$ ). BDE 209 contributed more than 90% to PBDEs in the NCP cities. Beijing is also an NCP city but had lower BDE-209 concentrations. This could be attributed to the APPCAP implementation, by which most heavy industries were moved out of Beijing. The highest BDE 209 level in the rural site of Shijiazhuang, the capital city of Hebei province, where most industries from Beijing were moved, was during winter at 1820  $pg/m^3$  and averaged at 478  $pg/m^3$ . In southern cities, BDE 28 and BDE 183 were the dominant PBDE congeners.

Guangzhou appeared to be the hotspot for NBFRs, featuring the highest DBDPE level among urban sites with an average of 384  $pg/m^3$  during winter, which is 1–2 orders of magnitude higher than that in other cities. Guangzhou also exhibited a high DP concentration of 52  $pg/m^3$ , which reflects that Guangdong province is the world's largest electronic manufacturing base with a long history of e-waste recycling.<sup>45,46</sup> There was a more consistent pattern observed across all sites for NBFRs, which was dominated by DBDPE (>80%).

OPFRs in this study were dominated by halo-OPFRs (>70%) with a more diverse intercity pattern. TDBPP was more prevalent in the northern sites, while TCPP and TCEP were more dominant in southern China. Lanzhou showed the highest OPFR concentrations. The Lanzhou "hotspot" for OPFRs could be a result of industrial transfer from east to west in China, accompanied by the movement of potential sources. For instance, industries such as textiles, manufacturing, electricity, etc. are the key FR emission sources. A shift-share analysis study indicated that the relocation of the pollution-intensive manufacturing industry in China was characterized by spatial movement from the east moving toward the west.<sup>47</sup> Furthermore, Lanzhou owns large-scale petrochemical industry and e-waste treatment sites were recently spotted there.<sup>48</sup>

**Temporal Trends.** The results of a 2013/2014 survey of FRs in atmospheric particles in Chinese cities are available for comparison.<sup>12</sup> We used these data to investigate temporal trends of selected FRs.  $\sum_7$  PBDEs, excluding BDE 154, were observed to drop, while BDE 209 increased slightly, as shown in Figure 3. The BDE 209 percentage increased from 35% to 43%, while that of BDE 28 decreased from 24% to 11% (Figure S7a). The decrease in PBDEs occurred slowly, which may be due to the continued emission into the atmosphere from numerous sources as indicated.<sup>49</sup> The increased levels of BDE 209 could be because of the recent deca-BDE mix ban in 2018, but it is still under the exemption period in China. A similar trend of decreased PBDEs (excluding BDE 209) along with increased

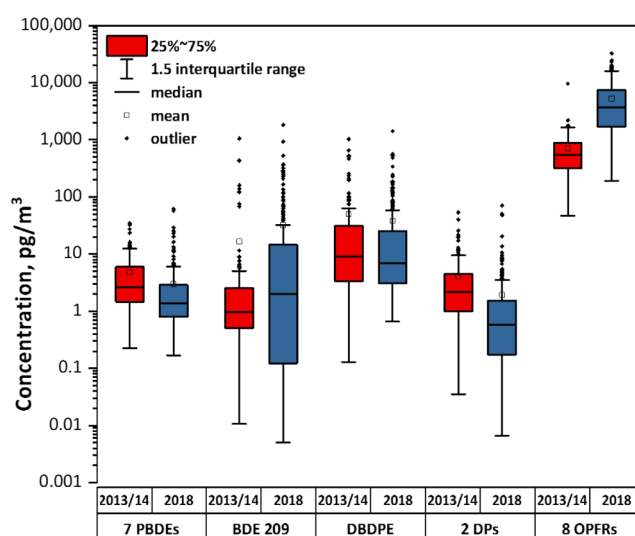


**Figure 3.** Temporal trends of selected FRs sampled between 2013/2014 and 2018.

BDE 209 has also been observed in the air of Chicago, which was shown to be mainly driven by emission from the household products used.<sup>49</sup>

Both DPs and NBFRs decreased by 50% and 20%, respectively, while the OPFR compounds increased by a factor of 5–10 between 2013/2014 and 2018, suggesting that they could be a potential FR alternative in China. A similar decrease in the NBFRs trend was also observed in the Antarctic atmosphere.<sup>7</sup> During these two sampling campaigns, the OPFRs composition was all dominated by TCPP and TCEP with total contributions >70%, as shown in Figure S7c. However, the DBDPE contribution greatly increased from 56% to 84%, and the average ratio of NBFRs/PBDEs increased from 3.5 to 5.1, which was largely due to the replacement of BDE 209.

**Influencing Factors. Socioeconomic Parameters.** In this study, there were significant correlations between most FRs, GDP, and the population living within a 20 km radius of the sampling sites (Table S14), similar to previous observations.<sup>28,50</sup> Notably, all PBDE congeners were not related to the disposal volume of industrial solid waste (Spearman  $r = -0.335 \sim -0.197$ ,  $p < 0.001$ ), while it was positively correlated with the storage capacity of industrial solid waste (except for BDE 209 and BDE 100) because the PBDE-containing products could not have reached the end of their lifecycles. Emissions from industrial and consumer chemicals, especially PBDEs, are expected to continue for decades beyond production termination because of their presence in long-lived durable goods and waste,<sup>51</sup> recently defined as "temporal environment hysteresis."<sup>49</sup> The exceptional BDE 209 case could be because of the exportation of most BDE 209 manufactured in China abroad<sup>51</sup> and possibly returned to China via e-waste import. It is estimated that more than 70% of PBDE emissions during waste disposal occurred before 2018 in less industrialized regions, as in China.<sup>25</sup>

**$PM_{2.5}$  and FR Concentrations.** The Spearman correlation between  $PM_{2.5}$  and FR volumetric concentration is summarized in Table S15. A significant positive correlation was found between the volumetric concentration of FRs ( $pg/m^3$ ) and particle concentration ( $\mu g/m^3$ ) for most FRs, indicating that the particle level could affect the atmospheric concentration of FRs in air, similar to observations in Beijing<sup>13</sup> and Dalian.<sup>20</sup>

Therefore, we hypothesized that a cobenefit was achieved by  $PM_{2.5}$  reduction with an average rate of  $-5 \mu\text{g}/\text{m}^3$  per year during 2013–2018 following the APPCAP implementation.<sup>52</sup> Relative humidity (RH) and precipitation were significantly negatively correlated to the FR volumetric concentration, suggesting that RH and precipitation could trigger stronger wet scavenging of particles in the atmosphere. The  $PM_{2.5}$ -bound fraction was also higher in winter than in summer, further supporting this inference (Figure S8 and S9).

To better understand the chemical composition of fine particles, we calculated the  $PM_{2.5}$ -normalized mass concentration of FRs ( $\text{pg}/\text{g } PM_{2.5}$ ) and investigated their relationship with meteorological parameters, as shown in Table S16. A significant negative correlation between  $PM_{2.5}$  mass-normalized concentrations of most FRs and  $PM_{2.5}$  in the air was identified, implying that more  $PM_{2.5}$  in the air may reduce the mass concentration of FRs in a single particle. Aerosol particles are emitted directly into the atmosphere (primary aerosol) and can be formed in the atmosphere (secondary aerosol, SA) via the chemical transformation of gaseous precursors.<sup>53</sup> Therefore, the negative correlation between  $PM_{2.5}$  mass-normalized concentrations of FRs and  $PM_{2.5}$  levels could be caused by the SA dilution effect, of which even secondary organic aerosol (SOA) could contribute between 30 and 77% of  $PM_{2.5}$  mass in the urban location of China and the percentage could still increase.<sup>54</sup> FRs, as semivolatile organic compounds (SVOC), are typical constituents of primary industrial and combustion sources.<sup>13,55</sup>

We also observed a significant negative relationship between FR mass concentration ( $\text{pg}/\text{g } PM_{2.5}$ ) and RH (Table S16). A similar phenomenon was previously observed in Beijing, where FR levels were reduced in foggy days with enhanced RH during APEC.<sup>13</sup> Because of an enhanced SA formation caused by aqueous oxidation under higher RH conditions, the FR fractions in the particulate phase were further diluted.<sup>56</sup>

**Gas-Particle Fractions.** Gas-particle partitioning is an essential environmental process governing atmospheric fate, wet/dry deposition, long-range transport, and their routes entering the human body.<sup>57,58</sup> In our results, the measured particle-bound fractions largely varied among different FRs (Figures S8 and S9). The particle-bound fraction of PBDEs ranged from BDE 28 at  $23 \pm 22\%$  to BDE 209 at  $71 \pm 34\%$ , and NBFs ranged from pentabromoethylbenzene (PBEB) at  $35 \pm 30\%$  to TBPH at  $70 \pm 27\%$ . OPFRs displayed a wider range of particle-bound fractions from tripropyl phosphate (TPPrP) at  $35 \pm 23\%$  to TEHP at  $85 \pm 19\%$ , owing to its wider spectrum of physicochemical properties. This particle-bound fraction is similar to the recently reported profile in Dalian<sup>20,21</sup> but different from those in the Bohai and Yellow seas,<sup>59</sup> Great Lakes,<sup>60</sup> and Antarctic.<sup>7,61</sup> Variable sources, particle level/composition, and environmental conditions could be responsible for this difference.<sup>59</sup> For example, it is reported that the particle-bound fractions tend to be higher in populated regions with higher particulate concentration compared to the remote region with lower particle level.<sup>19</sup> Significantly higher particle-bound fractions were found in winter than in summer for all FRs (except for triphenyl phosphate (TPhP) and TPPrP), as evidenced by the negative correlation between temperature and particle-bound fraction (Table S17), indicating that there is an effect of air temperature on SVOC gas-particle partition.

The measured G/P partition coefficient ( $\log K_{PM}$ ) and  $\log K_{OA}$  were positively correlated for most compounds (Table S18), suggesting that  $K_{OA}$  could be a predictor for the G/P partition behavior as expected.<sup>60</sup> At half of the urban sites, the

measured G/P coefficient ( $\log K_{PR}$ ) regression significantly correlated with  $\log K_{OA}$  (Figures 4 and S10). The predicted G/P

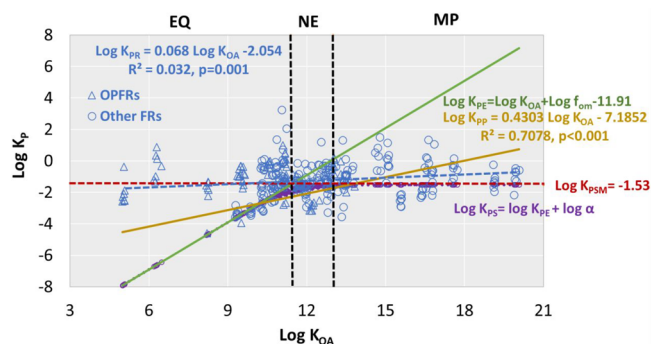


**Figure 4.** Log–log plots of  $K_{PR}$ ,  $K_{PP}$ , and  $K_{PE}$  and  $\log K_{PS}$  for all FRs in urban Shijiazhuang.  $\log K_{PR}$ , the regression of measured  $\log K_{PM}$  (blue hollow triangle for OPFRs and circle for other FRs), is shown using a blue dashed line.  $\log K_{PP}$  (yellow solid line),  $\log K_{PE}$  (green solid line), and  $\log K_{PS}$  (purple dots) were calculated using the corresponding G/P models. For  $\log K_{PS}$ , the left vertical black dashed line is the first  $\log K_{OA}$  threshold ( $\log K_{OA1} = 11.4$ ), dividing it into equilibrium domain (EQ) and nonequilibrium domain (NE), while the right vertical black dash is the second  $\log K_{OA}$  threshold ( $\log K_{OA2} = 13.0$ ) starting the maximum portioning (MP) domain.  $\log K_{PSM} = -1.53$  (the horizontal red dashed line) is the maximum constant value of  $\log K_{PS}$ .

coefficients using the mechanistic equations ( $\log K_{PP}$ ) worked better than the G/P coefficients predicted by the  $K_{OA}$ -based model ( $\log K_{PE}$ ) calculated by  $K_{OA}$ . The slopes of  $\log K_{PR}$  and  $\log K_{PP}$  varied among sites (Figure S10) but were all below unity, suggesting that the G/P partitioning of target FRs in Chinese cities could not have reached equilibrium. FRs in very fine and ultrafine particles could be possibly sampled and analyzed as the gas-phase fraction by high volume samplers, which has not been fully evaluated and could contribute to the observed nonequilibrium behavior.

The partitioning map was divided into three domains using two threshold  $\log K_{OA}$  values ( $\log K_{OA1} = 11.4$  and  $\log K_{OA2} = 13.0$ , defined as shown in Text S2) following the steady-state modeling approach.<sup>58</sup> The predicted G/P coefficient using the steady-state model ( $\log K_{PS}$ ) for compounds with a higher  $\log K_{OA}$  ( $>13.0$ ) was closer to the regression line of  $\log K_{PR}$ , suggesting that the G/P fractions are better suited with the steady-state model for chemicals with a higher  $\log K_{OA}$ , such as BDE 209, TDBPP, and TBPH. The largest deviation occurred in the EQ domain with  $\log K_{OA} < 11.4$  (Figure 4). In this study, the  $\log K_{PP}$  was closest to the  $\log K_{PR}$ , but the results calculated by using three models deviated from the observations, indicating that the FRs were far from equilibrium at the G/P interface. However, the deviation was mainly caused by FRs with lower  $\log K_{OA}$  values, such as triethyl phosphate (TEP,  $\log K_{OA} = 5.2$ ) and TCEP ( $\log K_{OA} = 8.3$ ), which are also more water-soluble (solubility  $5 \times 10^5$  and 7000 mg/L).<sup>62</sup> The sampling artifact could explain this phenomenon, in which a water film could form on quartz/glass filter fibers absorbing more hydrophilic OPFRs from the gaseous phase, leading to a concentration overestimation in the particulate phase.<sup>63</sup> Although, the hygroscopic nature of most SA constituents abundant in  $PM_{2.5}$  could also form an aqueous film on the particle, which could, in turn, capture more hydrophilic compounds from the gaseous phase, particularly under high RH conditions, as mentioned

above. Similar studies have also observed much higher OPFR fractions than expected in the particulate phase.<sup>59–61</sup>

**Challenges and Implications.** Our results demonstrated that OPFRs are abundant in Chinese air, comprising more than 95% of measured FRs across all sampling sites, OPFRs were first considered to be less persistent and bioaccumulative compared to the traditional FRs. Given this high exposure level, should they be reconsidered as a “regrettable substitution?”<sup>11</sup> Despite adequate risk assessments being lacking, recent studies have shown that these OPFRs can be degraded to more toxic mono- and diester OPFRs,<sup>64,65</sup> such as TPhP and diphenyl phosphate (DPHP).<sup>66,67</sup> The DPHP is generally used as an industrial catalyst and chemical additive and is also the primary aryl-OPFRs metabolite, whose sources have not been well-studied.<sup>66</sup> It has been further demonstrated to induce toxicity during embryonic development.<sup>66</sup> While there is limited information on the occurrence and behavior of OPFRs in ambient air, most relevant studies of mono- and diester OPFRs have so far focused on the indoor environment. Therefore, it is important to study their environmental behaviors, exposure pathways and metabolite toxicity.

Besides the conventional volumetric concentration ( $\text{pg}/\text{m}^3$ ), expressing chemical concentration using the unit of  $\text{PM}_{2.5}$  mass-normalized concentration ( $\text{pg}/\text{g PM}_{2.5}$ ) could have several advantages. When different units were used, various temporal trends were observed. For instance, an increasing temporal trend of PBDEs was observed between 2013/2014 and 2018 using  $\text{PM}_{2.5}$  mass-normalized concentration, while it was reduced when using volumetric concentration (Figure S11). First, the  $\text{PM}_{2.5}$  mass-based concentration could normalize and remove the effect of  $\text{PM}_{2.5}$  and atmospheric boundary layer height, which could vary among cities throughout the sampling. However, levels expressed using volumetric concentration ( $\text{pg}/\text{m}^3$ ) frequently increased linearly with  $\text{PM}_{2.5}$  levels and decreased as a power function of the atmospheric boundary layer height.<sup>68</sup> Second, when evaluating the effectiveness of the Stockholm Convention, a scenario could occur in which a city with better POPs control is found to have higher POPs in the air, largely owing to its higher particle levels. Third, the volumetric concentration of a target compound is often used to assess human exposure to POPs, but this could lead to inadequate health protection. The chemical level in a single particle, measured using  $\text{PM}_{2.5}$  mass-normalized concentration, could increase even if the volumetric concentration decreases, likely to lead to increased in situ toxicity of aerosol particles, as inferred from our data set. It was also reported that the  $\text{PM}_{2.5}$  mass-normalized concentration could be more helpful in obtaining results with the aim of protecting human health considering the toxicity property of the particles.<sup>69</sup>

A large knowledge gap exists regarding the possible interaction between highly particle-bound POPs (such as PBDEs) and SAs. SAs, including SOA and secondary inorganic aerosols (SIA), such as nitrates and sulfides, often dominate in  $\text{PM}_{2.5}$  or finer particles.<sup>70</sup> Therefore, we assume that the SA dominance on the particulate phase could cause a dilution effect on the POP concentrations because POPs are mainly from primary emissions. Further studies should be conducted to combine  $\text{PM}_{2.5}$ , SA, and POPs. It remains unclear if and how POPs and SOA/SIA interact with each other during G/P partitioning processes. The dynamic uptake of particulate POPs from the gaseous phase is very likely to happen because SA is newly formed, like on the absorbent of a passive air sampler.

Given that the system is kinetic, a dynamic uptake model could be more appropriate.

Most G/P partitioning measurement studies have so far focused on nonpolar or semipolar SVOC, such as PCBs and PBDEs.<sup>57,71</sup> However, emerging POPs, such as OPFRs, encompass a wide range of physicochemical properties.<sup>62</sup> These compounds with relatively higher water solubility may interact with SOA/SIA. For example, it was proposed that SVOC uptake into ambient SOA could be consistent with a kinetic condensation growth mechanism, indicating that the adsorbed SVOCs become incorporated into bulk particles as they are buried by the incoming gas molecules and do not re-evaporate.<sup>72</sup>

## ■ ASSOCIATED CONTENT

### Supporting Information

The Supporting Information is available free of charge at <https://pubs.acs.org/doi/10.1021/acs.est.0c07367>.

Detailed sampling information, instrumental methods, detection limits, FR concentrations summaries, comparison with literature, and additional results (PDF)

## ■ AUTHOR INFORMATION

### Corresponding Author

**Gan Zhang** – State Key Laboratory of Organic Geochemistry and Guangdong-Hong Kong-Macao Joint Laboratory for Environmental Pollution and Control, Guangzhou Institute of Geochemistry, Chinese Academy of Sciences, Guangzhou 510640, China; CAS Center for Excellence in Deep Earth Science, Guangzhou 510640, China; Guangdong Provincial Key Laboratory of Environmental Protection and Resources Utilization, Guangzhou 510640, China; [orcid.org/0000-0002-9010-8140](https://orcid.org/0000-0002-9010-8140); Email: [zhanggan@gig.ac.cn](mailto:zhanggan@gig.ac.cn)

### Authors

**Shizhen Zhao** – State Key Laboratory of Organic Geochemistry and Guangdong-Hong Kong-Macao Joint Laboratory for Environmental Pollution and Control, Guangzhou Institute of Geochemistry, Chinese Academy of Sciences, Guangzhou 510640, China; CAS Center for Excellence in Deep Earth Science, Guangzhou 510640, China; Guangdong Provincial Key Laboratory of Environmental Protection and Resources Utilization, Guangzhou 510640, China; [orcid.org/0000-0003-1534-9283](https://orcid.org/0000-0003-1534-9283)

**Lele Tian** – State Key Laboratory of Organic Geochemistry and Guangdong-Hong Kong-Macao Joint Laboratory for Environmental Pollution and Control, Guangzhou Institute of Geochemistry, Chinese Academy of Sciences, Guangzhou 510640, China; Guangdong Provincial Key Laboratory of Environmental Protection and Resources Utilization, Guangzhou 510640, China

**Zehao Zou** – School of Marine Sciences, Sun Yat-Sen University, Guangzhou 510275, China

**Xin Liu** – State Key Laboratory of Organic Geochemistry and Guangdong-Hong Kong-Macao Joint Laboratory for Environmental Pollution and Control, Guangzhou Institute of Geochemistry, Chinese Academy of Sciences, Guangzhou 510640, China; Guangdong Provincial Key Laboratory of Environmental Protection and Resources Utilization, Guangzhou 510640, China

**Guangcai Zhong** – State Key Laboratory of Organic Geochemistry and Guangdong-Hong Kong-Macao Joint

Laboratory for Environmental Pollution and Control, Guangzhou Institute of Geochemistry, Chinese Academy of Sciences, Guangzhou 510640, China; CAS Center for Excellence in Deep Earth Science, Guangzhou 510640, China; Guangdong Provincial Key Laboratory of Environmental Protection and Resources Utilization, Guangzhou 510640, China; [orcid.org/0000-0002-5647-5940](https://orcid.org/0000-0002-5647-5940)

**Yangzhi Mo** – State Key Laboratory of Organic Geochemistry and Guangdong-Hong Kong-Macao Joint Laboratory for Environmental Pollution and Control, Guangzhou Institute of Geochemistry, Chinese Academy of Sciences, Guangzhou 510640, China; Guangdong Provincial Key Laboratory of Environmental Protection and Resources Utilization, Guangzhou 510640, China; [orcid.org/0000-0002-6075-3421](https://orcid.org/0000-0002-6075-3421)

**Yan Wang** – Key Laboratory of Industrial Ecology and Environmental Engineering (MOE), School of Environmental Science and Technology, Dalian University of Technology, Dalian 116024, China; [orcid.org/0000-0003-0899-7899](https://orcid.org/0000-0003-0899-7899)

**Yankuan Tian** – State Key Laboratory of Organic Geochemistry and Guangdong-Hong Kong-Macao Joint Laboratory for Environmental Pollution and Control, Guangzhou Institute of Geochemistry, Chinese Academy of Sciences, Guangzhou 510640, China; Guangdong Provincial Key Laboratory of Environmental Protection and Resources Utilization, Guangzhou 510640, China

**Jun Li** – State Key Laboratory of Organic Geochemistry and Guangdong-Hong Kong-Macao Joint Laboratory for Environmental Pollution and Control, Guangzhou Institute of Geochemistry, Chinese Academy of Sciences, Guangzhou 510640, China; CAS Center for Excellence in Deep Earth Science, Guangzhou 510640, China; Guangdong Provincial Key Laboratory of Environmental Protection and Resources Utilization, Guangzhou 510640, China; [orcid.org/0000-0002-3637-1642](https://orcid.org/0000-0002-3637-1642)

**Hai Guo** – Department of Civil and Environmental Engineering, The Hong Kong Polytechnic University, Hong Kong, China; [orcid.org/0000-0002-7996-7294](https://orcid.org/0000-0002-7996-7294)

Complete contact information is available at:  
<https://pubs.acs.org/10.1021/acs.est.0c07367>

## Notes

The authors declare no competing financial interest.

## ACKNOWLEDGMENTS

This work was supported by the National Key R&D Program of China (2017YFC0212001), Guangdong Foundation for Program of Science and Technology Research (2017BT01Z134, 2019B121205006, 2019A1515011254, and 2017B030314057), Tuguangchi Award for Excellent Young Scholar GIG, and the State Key Laboratory of Organic Geochemistry, GIGCAS (SKLOG2020-9). We also greatly thank all volunteers who helped in the sampling campaign. We would like to express our sincere gratitude to Prof. Kevin Jones for his generously long-term help in promoting the monitoring of atmospheric POPs in China.

## REFERENCES

(1) Covaci, A.; Harrad, S.; Abdallah, M. A. E.; Ali, N.; Law, R. J.; Herzke, D.; de Wit, C. A. Novel brominated flame retardants: A review of their analysis, environmental fate and behaviour. *Environ. Int.* **2011**, *37* (2), 532–556.

(2) Proposal for a COUNCIL DECISION: on the Position to Be Adopted, on Behalf of the European Union, at the Eighth Conference of the Parties to the Stockholm Convention on Persistent Organic Pollutants Regarding the Proposals for Amendments of Annexes A and C; European Commission, 2017.

(3) Cooper, E. M.; Kroeger, G.; Davis, K.; Clark, C. R.; Ferguson, P. L.; Stapleton, H. M. Results from Screening Polyurethane Foam Based Consumer Products for Flame Retardant Chemicals: Assessing Impacts on the Change in the Furniture Flammability Standards. *Environ. Sci. Technol.* **2016**, *50* (19), 10653–10660.

(4) Abbasi, G.; Buser, A. M.; Soehl, A.; Murray, M. W.; Diamond, M. L. Stocks and Flows of PBDEs in Products from Use to Waste in the U.S. and Canada from 1970 to 2020. *Environ. Sci. Technol.* **2015**, *49* (3), 1521–1528.

(5) Stapleton, H. M.; Allen, J. G.; Kelly, S. M.; Konstantinov, A.; Klosterhaus, S.; Watkins, D.; McClean, M. D.; Webster, T. F. Alternate and New Brominated Flame Retardants Detected in U.S. House Dust. *Environ. Sci. Technol.* **2008**, *42* (18), 6910–6916.

(6) de Wit, C. A.; Herzke, D.; Vorkamp, K. Brominated flame retardants in the Arctic environment - trends and new candidates. *Sci. Total Environ.* **2010**, *408* (15), 2885–2918.

(7) Zhao, J.; Wang, P.; Wang, C.; Fu, M.; Li, Y.; Yang, R.; Fu, J.; Hao, Y.; Matsiko, J.; Zhang, Q.; Jiang, G. Novel brominated flame retardants in West Antarctic atmosphere (2011–2018): Temporal trends, sources and chiral signature. *Sci. Total Environ.* **2020**, *720*, 137557.

(8) Möller, A.; Xie, Z.; Cai, M.; Sturm, R.; Ebinghaus, R. Brominated Flame Retardants and Dechlorane Plus in the Marine Atmosphere from Southeast Asia toward Antarctica. *Environ. Sci. Technol.* **2012**, *46* (6), 3141–3148.

(9) Law, K.; Halldorson, T.; Danell, R.; Stern, G.; Gewurtz, S.; Alae, M.; Marvin, C.; Whittle, M.; Tomy, G. Bioaccumulation and trophic transfer of some brominated flame retardants in a Lake Winnipeg (Canada) food web. *Environ. Toxicol. Chem.* **2006**, *25* (8), 2177–2186.

(10) Sun, Y. X.; Luo, X. J.; Mo, L.; Zhang, Q.; Wu, J. P.; Chen, S. J.; Zou, F. S.; Mai, B. X. Brominated flame retardants in three terrestrial passerine birds from South China: Geographical pattern and implication for potential sources. *Environ. Pollut.* **2012**, *162*, 381–388.

(11) Blum, A.; Behl, M.; Birnbaum, L. S.; Diamond, M. L.; Phillips, A.; Singla, V.; Sipes, N. S.; Stapleton, H. M.; Venier, M. Organophosphate Ester Flame Retardants: Are They a Regrettable Substitution for Polybrominated Diphenyl Ethers? *Environ. Sci. Technol. Lett.* **2019**, *6* (11), 638–649.

(12) Liu, D.; Lin, T.; Shen, K.; Li, J.; Yu, Z.; Zhang, G. Occurrence and Concentrations of Halogenated Flame Retardants in the Atmospheric Fine Particles in Chinese Cities. *Environ. Sci. Technol.* **2016**, *50* (18), 9846–9854.

(13) Wang, T.; Tian, M.; Ding, N.; Yan, X.; Chen, S. J.; Mo, Y. Z.; Yang, W. Q.; Bi, X. H.; Wang, X. M.; Mai, B. X. Semivolatile Organic Compounds (SOCs) in Fine Particulate Matter (PM<sub>2.5</sub>) during Clear, Fog, and Haze Episodes in Winter in Beijing, China. *Environ. Sci. Technol.* **2018**, *52* (9), 5199–5207.

(14) Yang, M.; Qi, H.; Jia, H. L.; Ren, N. Q.; Ding, Y. S.; Ma, W. L.; Liu, L. Y.; Hung, H.; Sverko, E.; Li, Y. F. Polybrominated Diphenyl Ethers in Air across China: Levels, Compositions, and Gas-Particle Partitioning. *Environ. Sci. Technol.* **2013**, *47* (15), 8978–8984.

(15) Wu, D.; Xu, Y.; Zhang, S. Will joint regional air pollution control be more cost-effective? An empirical study of China's Beijing-Tianjin-Hebei region. *J. Environ. Manage.* **2015**, *149*, 27–36.

(16) Saini, A.; Harner, T.; Chinnadhurai, S.; Schuster, J. K.; Yates, A.; Sweetman, A.; Aristizabal-Zuluaga, B. H.; Jiménez, B.; Manzano, C. A.; Gaga, E. O.; Stevenson, G.; Falandysz, J.; Ma, J.; Miglioranza, K. S. B.; Kannan, K.; Tominaga, M.; Jariyasopit, N.; Rojas, N. Y.; Amador-Muñoz, O.; Sinha, R.; Alani, R.; Suresh, R.; Nishino, T.; Shoeib, T. GAPS-megacities: A new global platform for investigating persistent organic pollutants and chemicals of emerging concern in urban air. *Environ. Pollut.* **2020**, *267*, 115416.

(17) Zheng, Q.; Nizzetto, L.; Li, J.; Mulder, M. D.; Sáňka, O.; Lammel, G.; Bing, H.; Liu, X.; Jiang, Y.; Luo, C.; Zhang, G. Spatial Distribution of



Old and Emerging Flame Retardants in Chinese Forest Soils: Sources, Trends and Processes. *Environ. Sci. Technol.* **2015**, *49* (5), 2904–2911.

(18) Harner, T.; Bidleman, T. F. Octanol-air partition coefficient for describing particle/gas partitioning of aromatic compounds in urban air. *Environ. Sci. Technol.* **1998**, *32* (10), 1494–1502.

(19) Li, Y. F.; Qiao, L. N.; Ren, N. Q.; Sverko, E.; Mackay, D.; Macdonald, R. W. Decabrominated Diphenyl Ethers (BDE-209) in Chinese and Global Air: Levels, Gas/Particle Partitioning, and Long-Range Transport: Is Long-Range Transport of BDE-209 Really Governed by the Movement of Particles? *Environ. Sci. Technol.* **2017**, *51* (2), 1035–1042.

(20) Wang, Y.; Bao, M.; Tan, F.; Qu, Z.; Zhang, Y.; Chen, J. Distribution of organophosphate esters between the gas phase and PM<sub>2.5</sub> in urban Dalian, China. *Environ. Pollut.* **2020**, *259*, 113882.

(21) Wang, Y.; Zhang, Y.; Tan, F.; Yang, Y.; Qu, Z.; Kvasnicka, J.; Chen, J. Characteristics of halogenated flame retardants in the atmosphere of Dalian, China. *Atmos. Environ.* **2020**, *223*, 117219.

(22) Shi, S.; Huang, Y.; Wan, K.; Dong, L.; Yang, Y. Levels and Seasonal Variations of Polybrominated Diphenyl Ethers in the Urban Atmosphere of Beijing, China. *Bull. Environ. Contam. Toxicol.* **2013**, *90* (3), 296–301.

(23) Syed, J. H.; Iqbal, M.; Breivik, K.; Chaudhry, M. J. I.; Shah Nawaz, M.; Abbas, Z.; Nasir, J.; Rizvi, S. H. H.; Taqi, M. M.; Li, J.; Zhang, G. Legacy and emerging flame retardants (FRs) in the urban atmosphere of Pakistan: Diurnal variations, gas-particle partitioning and human health exposure. *Sci. Total Environ.* **2020**, *743*, 140874.

(24) Liu, L. Y.; Salamova, A.; Venier, M.; Hites, R. A. Trends in the levels of halogenated flame retardants in the Great Lakes atmosphere over the period 2005–2013. *Environ. Int.* **2016**, *92–93*, 442–449.

(25) Abbasi, G.; Li, L.; Breivik, K. Global Historical Stocks and Emissions of PBDEs. *Environ. Sci. Technol.* **2019**, *53* (11), 6330–6340.

(26) Shen, K. H.; Li, L.; Liu, J. Z.; Chen, C. K.; Liu, J. G. Stocks, flows and emissions of DBDPE in China and its international distribution through products and waste. *Environ. Pollut.* **2019**, *250*, 79–86.

(27) Investigation Report of Flame Retardant Area from 2013 to 2015; China Fire Retardant Chemical Association, 2015 (in Chinese).

(28) Ma, Y.; Salamova, A.; Venier, M.; Hites, R. A. Has the Phase-Out of PBDEs Affected Their Atmospheric Levels? Trends of PBDEs and Their Replacements in the Great Lakes Atmosphere. *Environ. Sci. Technol.* **2013**, *47* (20), 11457–11464.

(29) Ji, X.; Xie, X.; Ding, J.; Cheng, Y.; He, H.; Huang, Y.; Qin, L.; Zhu, H.; Zhao, C.; Li, A.; Han, C. Chlorinated flame retardant Dechlorane Plus: environmental pollution in China. *Environ. Rev.* **2018**, *26* (3), 273–285.

(30) Ren, N.; Sverko, E.; Li, Y. F.; Zhang, Z.; Harner, T.; Wang, D.; Wan, X.; McCarry, B. E. Levels and Isomer Profiles of Dechlorane Plus in Chinese Air. *Environ. Sci. Technol.* **2008**, *42* (17), 6476–6480.

(31) Li, W. L.; Liu, L. Y.; Song, W. W.; Zhang, Z. F.; Qiao, L. N.; Ma, W. L.; Li, Y. F. Five-year trends of selected halogenated flame retardants in the atmosphere of Northeast China. *Sci. Total Environ.* **2016**, *539*, 286–293.

(32) Schuster, J. K.; Harner, T.; Sverko, E. Dechlorane Plus in the Global Atmosphere. *Environ. Sci. Technol. Lett.* **2021**, *8* (1), 39–45.

(33) Salamova, A.; Hermanson, M. H.; Hites, R. A. Organophosphate and Halogenated Flame Retardants in Atmospheric Particles from a European Arctic Site. *Environ. Sci. Technol.* **2014**, *48* (11), 6133–6140.

(34) Wang, D. G.; Yang, M.; Qi, H.; Sverko, E.; Ma, W. L.; Li, Y. F.; Alaei, M.; Reiner, E. J.; Shen, L. An Asia-Specific Source of Dechlorane Plus: Concentration, Isomer Profiles, and Other Related Compounds. *Environ. Sci. Technol.* **2010**, *44* (17), 6608–6613.

(35) Zhang, W.; Wang, P.; Li, Y.; Wang, D.; Matsiko, J.; Yang, R.; Sun, H.; Hao, Y.; Zhang, Q.; Jiang, G. Spatial and temporal distribution of organophosphate esters in the atmosphere of the Beijing-Tianjin-Hebei region, China. *Environ. Pollut.* **2019**, *244*, 182–189.

(36) Yaman, B.; Dumanoglu, Y.; Odabasi, M. Measurement and Modeling the Phase Partitioning of Organophosphate Esters Using Their Temperature-Dependent Octanol-Air Partition Coefficients and Vapor Pressures. *Environ. Sci. Technol.* **2020**, *54* (13), 8133–8143.

(37) Wong, F.; de Wit, C. A.; Newton, S. R. Concentrations and variability of organophosphate esters, halogenated flame retardants, and polybrominated diphenyl ethers in indoor and outdoor air in Stockholm, Sweden. *Environ. Pollut.* **2018**, *240*, 514–522.

(38) Prival, M. J.; McCoy, E. C.; Gutter, B.; Rosendranz, H. S. Tris(2,3-dibromopropyl) phosphate: mutagenicity of a widely used flame retardant. *Science* **1977**, *195* (4273), 76.

(39) Dodson, R. E.; Perovich, L. J.; Covaci, A.; Van den Eede, N.; Ionas, A. C.; Dirtu, A. C.; Brody, J. G.; Rudel, R. A. After the PBDE Phase-Out: A Broad Suite of Flame Retardants in Repeat House Dust Samples from California. *Environ. Sci. Technol.* **2012**, *46* (24), 13056–13066.

(40) Peeverly, A. A.; Salamova, A.; Hites, R. A. Air is Still Contaminated 40 Years after the Michigan Chemical Plant Disaster in St. Louis, Michigan. *Environ. Sci. Technol.* **2014**, *48* (19), 11154–11160.

(41) Allan, I. J.; Garmo, Ø. A.; Rundberget, J. T.; Terentjev, P.; Christensen, G.; Kashulin, N. A. Detection of tris(2,3-dibromopropyl) phosphate and other organophosphorous compounds in Arctic rivers. *Environ. Sci. Pollut. Res.* **2018**, *25* (28), 28730–28737.

(42) Li, J.; Xie, Z.; Mi, W.; Lai, S.; Tian, C.; Emeis, K. C.; Ebinghaus, R. Organophosphate Esters in Air, Snow, and Seawater in the North Atlantic and the Arctic. *Environ. Sci. Technol.* **2017**, *51* (12), 6887–6896.

(43) Gold, M. D.; Blum, A.; Ames, B. N. Another Flame-Retardant, Tris-(1,3-Dichloro-2-Propyl)-Phosphate, and Its Expected Metabolites Are Mutagens. *Science* **1978**, *200* (4343), 785–787.

(44) An, Z.; Huang, R. J.; Zhang, R.; Tie, X.; Li, G.; Cao, J.; Zhou, W.; Shi, Z.; Han, Y.; Gu, Z.; Ji, Y. Severe haze in northern China: A synergy of anthropogenic emissions and atmospheric processes. *Proc. Natl. Acad. Sci. U. S. A.* **2019**, *116* (18), 8657.

(45) Tian, M.; Chen, S. J.; Wang, J.; Zheng, X. B.; Luo, X. J.; Mai, B. X. Brominated Flame Retardants in the Atmosphere of E-Waste and Rural Sites in Southern China: Seasonal Variation, Temperature Dependence, and Gas-Particle Partitioning. *Environ. Sci. Technol.* **2011**, *45* (20), 8819–8825.

(46) Li, Q.; Yang, K.; Li, K.; Liu, X.; Chen, D.; Li, J.; Zhang, G. New halogenated flame retardants in the atmosphere of nine urban areas in China: Pollution characteristics, source analysis and variation trends. *Environ. Pollut.* **2017**, *224*, 679–688.

(47) Zuo, Y.; Heng, C. The Research on Relocation of China's Pollution-intensive Manufacturing Industry based on Shift-share Analysis. *Journal of Gansu Administration Institute* **2020**, *2*, 98–127.

(48) Cao, H.; Li, Y.; Li, Z. L.; Zhao, L. Z.; Mao, X.; Mu, X.; Huang, T.; Gao, H.; Ma, J. Occurrence And Occupational Risk Of Polybrominated Diphenyl Ethers (PBDEs) And Dechlorane Plus (DP) In A Formal E-Waste Recycling Plant, Northwest China. *Journal of Environmental Science Current Research* **2019**, S2001.

(49) Hites, R. A.; Lehman, D. C.; Salamova, A.; Venier, M. Temporal environmental hysteresis: A definition and implications for polybrominated diphenyl ethers. *Sci. Total Environ.* **2021**, *753*, 141849.

(50) Li, W. L.; Qi, H.; Ma, W. L.; Liu, L. Y.; Zhang, Z.; Mohammed, M. O. A.; Song, W. W.; Zhang, Z.; Li, Y. F. Brominated flame retardants in Chinese air before and after the phase out of polybrominated diphenyl ethers. *Atmos. Environ.* **2015**, *117*, 156–161.

(51) Li, L.; Wania, F. Occurrence of Single- and Double-Peaked Emission Profiles of Synthetic Chemicals. *Environ. Sci. Technol.* **2018**, *52* (8), 4684–4693.

(52) Zhai, S.; Jacob, D. J.; Wang, X.; Shen, L.; Li, K.; Zhang, Y.; Gui, K.; Zhao, T.; Liao, H. Fine particulate matter (PM<sub>2.5</sub>) trends in China, 2013–2018: separating contributions from anthropogenic emissions and meteorology. *Atmos. Chem. Phys.* **2019**, *19* (16), 11031–11041.

(53) Pöschl, U. Atmospheric Aerosols: Composition, Transformation, Climate and Health Effects. *Angew. Chem., Int. Ed.* **2005**, *44* (46), 7520–7540.

(54) Huang, R. J.; Zhang, Y.; Bozzetti, C.; Ho, K. F.; Cao, J. J.; Han, Y.; Daellenbach, K. R.; Slowik, J. G.; Platt, S. M.; Canonaco, F.; Zotter, P.; Wolf, R.; Pieber, S. M.; Bruns, E. A.; Crippa, M.; Ciarelli, G.; Piazzalunga, A.; Schwikowski, M.; Abbazade, G.; Schnelle-Kreis, J.; Zimmermann, R.; An, Z.; Szidat, S.; Baltensperger, U.; Haddad, I. E.;

Prévôt, A. S. H. High secondary aerosol contribution to particulate pollution during haze events in China. *Nature* **2014**, *514* (7521), 218–222.

(55) Wang, L. C.; Lee, W. J.; Lee, W. S.; Chang-Chien, G. P. Polybrominated diphenyl ethers in various atmospheric environments of Taiwan: Their levels, source identification and influence of combustion sources. *Chemosphere* **2011**, *84* (7), 936–942.

(56) Du, Z.; He, K.; Cheng, Y.; Duan, F.; Ma, Y.; Liu, J.; Zhang, X.; Zheng, M.; Weber, R. A yearlong study of water-soluble organic carbon in Beijing I: Sources and its primary vs. secondary nature. *Atmos. Environ.* **2014**, *92*, 514–521.

(57) Qiao, L. N.; Hu, P. T.; Macdonald, R.; Kannan, K.; Nikolaev, A.; Li, Y. F. Modeling gas/particle partitioning of polybrominated diphenyl ethers (PBDEs) in the atmosphere: A review. *Sci. Total Environ.* **2020**, *729*, 138962.

(58) Li, Y. F.; Ma, W. L.; Yang, M. Prediction of gas/particle partitioning of polybrominated diphenyl ethers (PBDEs) in global air: A theoretical study. *Atmos. Chem. Phys.* **2015**, *15* (4), 1669–1681.

(59) Li, J.; Tang, J.; Mi, W.; Tian, C.; Emeis, K. C.; Ebinghaus, R.; Xie, Z. Spatial Distribution and Seasonal Variation of Organophosphate Esters in Air above the Bohai and Yellow Seas, China. *Environ. Sci. Technol.* **2018**, *52* (1), 89–97.

(60) Wu, Y.; Venier, M.; Salamova, A. Spatioseasonal Variations and Partitioning Behavior of Organophosphate Esters in the Great Lakes Atmosphere. *Environ. Sci. Technol.* **2020**, *54* (9), 5400–5408.

(61) Wang, C.; Wang, P.; Zhao, J.; Fu, M.; Zhang, L.; Li, Y.; Yang, R.; Zhu, Y.; Fu, J.; Zhang, Q.; Jiang, G. Atmospheric organophosphate esters in the Western Antarctic Peninsula over 2014–2018: Occurrence, temporal trend and source implication. *Environ. Pollut.* **2020**, *267*, 115428.

(62) Wang, X.; Zhu, Q.; Yan, X.; Wang, Y.; Liao, C.; Jiang, G. A review of organophosphate flame retardants and plasticizers in the environment: Analysis, occurrence and risk assessment. *Sci. Total Environ.* **2020**, *731*, 139071.

(63) Okeme, J. O.; Rodgers, T. F. M.; Jantunen, L. M.; Diamond, M. L. Examining the Gas-Particle Partitioning of Organophosphate Esters: How Reliable Are Air Measurements? *Environ. Sci. Technol.* **2018**, *52* (23), 13834–13844.

(64) Tan, H.; Yang, L.; Yu, Y.; Guan, Q.; Liu, X.; Li, L.; Chen, D. Co-Existence of Organophosphate Di- and Tri-Esters in House Dust from South China and Midwestern United States: Implications for Human Exposure. *Environ. Sci. Technol.* **2019**, *53* (9), 4784–4793.

(65) Wang, L.; Jia, Y.; Kang, Q.; Song, W.; Hu, J. Nontarget Discovery of 11 Aryl Organophosphate Triesters in House Dust Using High-Resolution Mass Spectrometry. *Environ. Sci. Technol.* **2020**, *54* (18), 11376–11385.

(66) Mitchell, C. A.; Reddam, A.; Dasgupta, S.; Zhang, S.; Stapleton, H. M.; Volz, D. C. Diphenyl Phosphate-Induced Toxicity During Embryonic Development. *Environ. Sci. Technol.* **2019**, *53* (7), 3908–3916.

(67) Li, Y.; Kang, Q.; Chen, R.; He, J.; Liu, L.; Wang, L.; Hu, J. 2-Ethylhexyl Diphenyl Phosphate and Its Hydroxylated Metabolites are Anti-androgenic and Cause Adverse Reproductive Outcomes in Male Japanese Medaka (*Oryzias latipes*). *Environ. Sci. Technol.* **2020**, *54* (14), 8919–8925.

(68) Cao, R.; Zhang, H.; Zhao, L.; Zhang, Y.; Geng, N.; Teng, M.; Zou, L.; Gao, Y.; Ni, Y.; Fu, Q.; Chen, J. Hazy Weather-Induced Variation in Environmental Behavior of PCDD/Fs and PBDEs in Winter Atmosphere of A North China Megacity. *Environ. Sci. Technol.* **2018**, *52* (15), 8173–8182.

(69) Li, J.; Chen, H.; Li, X.; Wang, M.; Zhang, X.; Cao, J.; Shen, F.; Wu, Y.; Xu, S.; Fan, H.; Da, G.; Huang, R.-j.; Wang, J.; Chan, C. K.; De Jesus, A. L.; Morawska, L.; Yao, M. Differing toxicity of ambient particulate matter (PM) in global cities. *Atmos. Environ.* **2019**, *212*, 305–315.

(70) Robinson, A. L.; Donahue, N. M.; Shrivastava, M. K.; Weitkamp, E. A.; Sage, A. M.; Grieshop, A. P.; Lane, T. E.; Pierce, J. R.; Pandis, S. N. Rethinking Organic Aerosols: Semivolatile Emissions and Photochemical Aging. *Science* **2007**, *315* (5816), 1259–1262.

(71) Wang, P.; Li, Y.; Zhang, Q.; Yang, Q.; Zhang, L.; Liu, F.; Fu, J.; Meng, W.; Wang, D.; Sun, H.; Zheng, S.; Hao, Y.; Liang, Y.; Jiang, G. Three-year monitoring of atmospheric PCBs and PBDEs at the Chinese Great Wall Station, West Antarctica: Levels, chiral signature, environmental behaviors and source implication. *Atmos. Environ.* **2017**, *150*, 407–416.

(72) Perraud, V.; Bruns, E. A.; Ezell, M. J.; Johnson, S. N.; Yu, Y.; Alexander, M. L.; Zelenyuk, A.; Imre, D.; Chang, W. L.; Dabdub, D.; Pankow, J. F.; Finlayson-Pitts, B. J. Nonequilibrium atmospheric secondary organic aerosol formation and growth. *Proc. Natl. Acad. Sci. U. S. A.* **2012**, *109* (8), 2836–2841.